

Strength and Constitutive Model of Chromium-contaminated Soil after Combined Remediation

Ling Liu^{1,*}, Zhongkai Tong¹, Xilin Li¹ and Dan Meng²

¹School of Civil Engineering, Liaoning Technical University, Fuxin 123000, Liaoning, China

²School of Built Environment, University of New South Wales, Sydney 2052, NSW, Australia

Received 19 January 2022; Accepted 1 May 2022

Abstract

Heavy metal-contaminated soil has become an influencing factor that restricts environmental development. Remediation of contaminated soil and use of the repaired soil for other purposes are of great practical significance. The constitutive relationship of solidified soil is important to evaluate the strength and mechanical properties of deformation. Understanding the constitutive relationship of solidified soil is the basis for applying it to roadbed filling or building materials. This study used contaminated soil repaired by calcium polysulfide, synthetic zeolite from fly ash, and cement as research objects. The strength characteristics of the solidified soil under different water contents, chromium concentrations, and curing ages were determined through indoor tests. The stress-strain curve of the solidified soil under different conditions was obtained. The necessity of introducing damage variables was analyzed. The damage variable was introduced based on the *Popovics* model, and an improved constitutive model of the solidified soil was established. The constitutive model was then compared with the test results to validate the established model. Results show that the strength of the solidified soil is positively correlated with curing ages and negatively correlated with chromium concentrations. The unconfined compressive strength (UCS) of the solidified soil after 7 days of curing is the highest at the water content of 22%, while that after 28 days of curing is negatively correlated with water contents. The established model can describe the entire strain deformation process of solidified soil under different water contents, curing ages, and chromium concentrations. This model can fully reflect the linear elastic deformation characteristics of the solidified soil at the initial stage and the subsequent nonlinear mechanical behavior. The simulation results verify the rationality of the established model. The obtained conclusions provide a significantly reference for the engineering application of solidified heavy metal-contaminated soil.

Keywords: Chromium-contaminated soil, Synthetic zeolite from fly ash, Cement, Damage variable, Constitutive model

1. Introduction

Heavy metal-contaminated soils are widely distributed all over the world, causing great harm to ecosystems and people's health. The number of underground structures gradually increases with the development and utilization of urban underground space. The presence of heavy metal ions can reduce the stability and durability of underground engineering structures and facilities, thereby affecting the actual life of the project [1]. Chromium-contaminated soil is characterized by strong toxicity, persistence, complexity, and irreversibility, and its pollution remediation has become a very urgent problem. High concentrations of chromium can reduce the strength and bearing capacity of solidified soil, causing more serious safety hazards [2]. Therefore, corresponding measures must be taken to repair chromium-contaminated soil to meet the needs of production and construction or the requirements of roadbed fillings and building materials.

At present, solidification/stabilization (S/S) method is mainly used to repair heavy metal-contaminated soil at home and abroad; it not only avoids groundwater pollution by heavy metals but also improves the strength of the soil and meets the engineering needs. Heavy metal-contaminated soil

repaired by S/S method can be used as roadbed fillings and building materials [3]. However, S/S method alone cannot completely treat soil contaminated by high concentrations of heavy metals. Fitch et al. [4] monitored the long-term engineering characteristics of heavy metal-contaminated sites solidified by cement and fly ash after 10 years. The surface soil of about 50 mm thickness was severely degraded, the strength was significantly reduced, and the contents of heavy metal ions increased. For soil contaminated by high concentrations of chromium, considering that the toxicity of Cr(III) is lower than that of Cr(VI), CaS_x can be used to reduce Cr(VI) into Cr(III), synthetic zeolite prepared from waste fly ash is then used to adsorb Cr(III), and chromium pollutants are fixed through cement solidification [5]. In this method, chromium-contaminated soil can be effectively repaired. To realize waste reuse, scholars have explored the use of chromium-contaminated soil after combined remediation as roadbed fillings.

The key to using repaired contaminated soil as roadbed fillings is that its mechanical properties should meet the requirements of corresponding uses. Therefore, the influence of different factors on the unconfined compressive strength (UCS) of contaminated soil after remediation should be investigated. Results provide a basis for the application of repaired chromium-contaminated soil in engineering. The mechanical properties of chromium-contaminated soil

*E-mail address: liuling@lntu.edu.cn

ISSN: 1791-2377 © 2022 School of Science, IHU. All rights reserved.

doi:10.25103/jestr.151.06

repaired by composite preparation are different from those of general natural soils and rocks; as such, the constitutive relations of repaired soils cannot simply follow the constitutive relations of conventional soils. It is necessary to analyze the uniaxial test results and establish a constitutive model that conforms to the characteristics of the chromium-contaminated soil after combined remediation by the solidification-reduction-adsorption.

Based on this, according to the stress-strain curves obtained under the conditions of different water contents, chromium concentrations, and curing ages, the damage variable is introduced, and an improved constitutive model of the solidified body is established. This work aims to lay a foundation for further research and application of the solidified body of contaminated soil.

2. State of the art

The constitutive theory of geotechnical materials is the foundation of modern geotechnical mechanics. It is of great practical significance to study the stress-strain relationship of heavy metal-solidified soil, and to establish the constitutive model of heavy metal solidified soil, for using the repaired contaminated soil as roadbed fillings and building materials. At present, domestic and foreign scholars conducted research on the constitutive model of solidified soil mainly by using cement and conventional soil as the research object. The models include damage constitutive model, elastoplastic constitutive model, elastoplastic damage constitutive model, and constitutive model which considers the structure of solidified soil [6-8]. Chong et al. [9] proposed a cement-soil constitutive model to describe the volume change of soil stiffness and strength related to pressure and used it to simulate the triaxial drainage test. The initial isotropic stress state and the degradation rate of cement determined the stress-strain volume response of cement. Zhi et al. [10] established a constitutive model of structured loess under high-stress conditions based on the binary-medium model and homogenization theory. The constitutive model parameters of structural loess were determined through triaxial compression tests. The comparison of the calculation and test results verified the rationality of the established constitutive model. Tu et al. [11] established a two-stage constitutive model of cemented tailings backfill based on Weibull distribution density function, strain equivalence principle, and damage mechanics theory. The rationality of the model was verified through experiments. The destruction mode of the specimen under uniaxial compression was mainly tensile destruction. Yao et al. [12] proposed a simple constitutive model to describe the mechanical behavior of granular soil in a large stress range. This model could describe the hardening process of the yield surface. Bathayian et al. [13] proposed an elastoplastic constitutive model suitable for granular soil to describe the stress-strain characteristics of cemented granular soil.

Some scholars have also studied the constitutive models of frozen soil, sandstone, and cementing materials. Wang et al. [14] established a macro-micro creep constitutive model with visco-elastoplastic deformation characteristics of three-phase frozen soil. The model parameters were determined by creep test based on frozen soil, and the model was verified by the creep test results of saturated frozen soil. The model could well reflect the influence of temperature and ice contents on the creep of saturated frozen soil. Pan et al. [15]

studied the deformation behavior of rocks during compression. A non-linear statistical damage constitutive model was established using the method based on statistical damage. The model fitted well for rocks of different types, confining pressures, and water contents. This model could be applied to most rock types and in most engineering environments. Scholars also consider the processes of damage evolution and ice volume evolution when studying the constitutive model of frozen soil [16,17]. Abioghli et al. [18] established a constitutive model to predict the mechanical properties of fiber-reinforced cemented sand. They revised the elastic parameters, flow laws, and hardening laws of the model and verified the effectiveness of the model through experiments. Doherty et al. [19] proposed a constitutive model that could reflect the formation and destruction of weakly cemented granular materials under transient stress environments. In addition, some constitutive models were studied considering different factors, including dilatancy effect, brittle cracking, plastic rebound, and other factors [20-22].

Existing research mainly focuses on the constitutive relationship models of various conventional soils and sandstone cementing materials. However, few studies have investigated the constitutive model and relationship of solidified contaminated soil and the stress-strain relationship of the contaminated soil after solidification and remediation. In particular, the constitutive model of solidified heavy metal-contaminated soil has not been reported yet.

Aiming at the shortcomings of existing research, the present work focused on chromium-contaminated soil after remediation by composite preparation. The effects of different water contents, chromium concentrations, and curing ages on the UCS of the solidified soil were studied. The stress-strain curves of the solidified soil under different conditions were obtained. Based on the curves, an improved constitutive model of solidified contaminated soil was established, and the rationality of the model was verified. Results can lay the foundation for the application of contaminated soil after remediation to engineering practice.

The rest of this study is organized as follows. Section 3 describes test materials and methodology. Section 4 analyzes the strength characteristics and the stress-strain relationship and establishes a full-stage stress-strain model. Section 5 summarizes the study and presents relevant conclusions.

3. Methodology

3.1 Test material and its composition

The CaS_x used in the experiment has a volume fraction of 29% and its main component is CaS_5 (China Lianyungang Lanxing Industrial Technology Co., Ltd.). The chemical composition of P.O42.5-grade Portland cement produced in Fuxin is shown in Table 1. Synthetic zeolite was prepared through alkali fusion-hydrothermal method using fly ash [23], and its chemical composition is also shown in Table 1. Taking into account the heterogeneity and complexity of the original contaminated soil, soil was collected from an uncontaminated area 2 km away from the Shenyang chromium-contaminated site. The soil is silty clay and has maximum dry density of 1.72 g/cm³, and the optimal moisture content of 22.0%. Other chemical components and physical properties of soil are shown in Tables 1 and 2. Debris was removed from the clay, which was then passed through a 2 mm sieve and air dried naturally. A solution

with certain mass concentration was prepared by K_2CrO_4 and $CrNO_3$, then mixed with the sieved soil to prepare chromium-contaminated soil with different Cr(VI) and

Cr(III) concentrations. Distilled water was used as test water. All reagents used are analytically pure.

Table 1. Chemical composition of silty clay, synthetic zeolite from fly ash and cement (mass fraction/%)

Chemical composition	SiO ₂	Al ₂ O ₃	CaO	MgO	Fe ₂ O ₃	K ₂ O	Na ₂ O	TiO ₂	SO ₃	Ignition loss	P ₂ O ₅
Silty clay	53.1	31.2	1.7	0.9	1.6	1.3	3.6	-	-	-	0.6
Portland cement	21.87	5.69	62.25	3.12	3.80	1.41	0.35	-	1.02	0.48	-
Synthetic zeolite	50.29	14.17	3.42	1.96	7.23	1.05	20.88	0.55	-	-	-

Table 2. Physical properties of silty clay

Index	Natural density /g·cm ⁻¹	Proportion	Saturation /%	Liquid limit /%	Plastic limit /%	Plastic Limit Index	Void ratio	Particle composition (by weight) /%	
								Sand	Cosmid
Value	1.99	2.71	91.3	30.6	18.7	11.9	0.657	42	32

Table 3. Proportioning schemes of test pieces

Experimental group	Cr(VI) contents/mg·kg ⁻¹	Chromium-contaminated soil/g	CaS _x /multiple	Synthetic zeolite/g	Cement/g	Water/mL
A1	3000	260	3	60	80	72
A2	3000	260	3	60	80	80
A3	3000	260	3	60	80	88
A4	3000	260	3	60	80	96
A5	3000	260	3	60	80	104
B1	500	260	3	60	80	88
B2	1000	260	3	60	80	88
B3	3000	260	3	60	80	88
B4	5000	260	3	60	80	88
B5	10000	260	3	60	80	88

3.2 Specimen design and preparation

In this experiment, 10 groups of proportion schemes were designed (Table 3). Specimens were prepared according to the ratio in the table and cured for 28 days. Three parallel specimens were prepared for each group. The effects of different water contents and chromium concentrations on the strength of chromium-contaminated soil after remediation were investigated. With the A3 scheme as the benchmark mix ratio, six groups of specimens were prepared to investigate the influence of different curing ages (7, 14, 28, 56, 84, and 180 days) on the strength of chromium-contaminated soil after remediation.

In this experiment, 16 groups of specimens of chromium-contaminated soil after combined remediation were produced. Each group contains three parallel specimens, which adds up to a total of 48 specimens. The specimen is a cylinder with the dimension of ϕ 50 mm×100 mm. The order of adding various materials during the production of the specimen is as follows.

According to the ratio in Table 3, CaS_x and water (22% of the mass of soil) were firstly added to the contaminated soil, mixed, and stirred for 30 min. The sample was secondly added with synthetic zeolite and water (22% of the mass of zeolite), mixed, and stirred for 30 min. The sample was then added with cement and water (22% of the cement mass), mixed, and stirred for 10 min to obtain repaired soil. Static pressure method was finally used to prepare standard specimens. The specimens were placed in a standard curing room with temperature of (20±2) °C and relative humidity above 95% for 28 days of curing.

3.3 Test device and loading plan

Uniaxial compression test was carried out using a compression testing machine. The loading process was controlled by displacement, and the loading speed was 0.1 mm/min. Each group used three identical specimens for

repeated test under the same stress state to ensure the repeatability of the test. The operation procedure is referred to ASTM D2166-06.

4 Experimental results and Analysis

4.1 Characteristic analysis of strength

The specimens were prepared according to different water contents and chromium concentrations in Table 3. After curing for 28 days, UCS was determined. Taking the A3 mix ratio as the reference mix ratio, UCS was measured after curing for 7, 14, 28, 56, 84, and 180 days. The test results are shown in Fig. 1.

From Fig. 1a, increasing chromium concentrations can gradually reduce the strength of the solidified body. When the chromium concentrations are low, CaS_x in the composite preparation can completely convert Cr(VI) into Cr(III), and the synthetic zeolite can completely adsorb Cr(III). Therefore, chromium ions have little interference with the hydration and pozzolanic reactions of the cement, and the strength of the solidified body is high. However, CaS_x and synthetic zeolite are less effective in reducing and adsorbing high-concentration pollutants. Free chromium ions hinder the hydration and pozzolanic reactions of cement and increase the weakening effect on the strength of the solidified soil, resulting in a decrease in the strength of the solidified soil [24].

As the curing ages increase, the strength of the solidified soil also increases (Fig. 1b). For the chromium-contaminated soil repaired by composite preparation, CaS_x and synthetic zeolite greatly reduce the hindering effect of Cr(VI) and Cr(III) on the hydration and pozzolanic reactions. The reaction time of active SiO₂ and Al₂O₃ in the synthetic zeolite from fly ash is relatively late, thereby increasing the strength of the solidified body [25].

When the specimen was cured for 7 days, the maximum strength value appeared at the optimal water content of 22% (Fig. 1c). After curing for 7 days, Cr(III) in the contaminated soil and the unreduced Cr(VI) jointly delay the hydration and pozzolanic reactions, and the composite preparation has not fully exerted its solidified effect. After curing for 28 days, as the water contents increase within a certain range, the strength of the solidified body decreases. On the one hand, when the water contents are high, the remaining water in the solidified body makes the hydration film of the soil

particles too thick, resulting in a decrease in strength. On the other hand, higher water contents are conducive to the full contact and reaction between Cr(VI) in contaminated soil and CaS₅ in composite preparation. More Cr(VI) is reduced into Cr(III), which has a more obvious weakening effect on the UCS of the solidified body. Therefore, high water contents have a negative impact on strength.

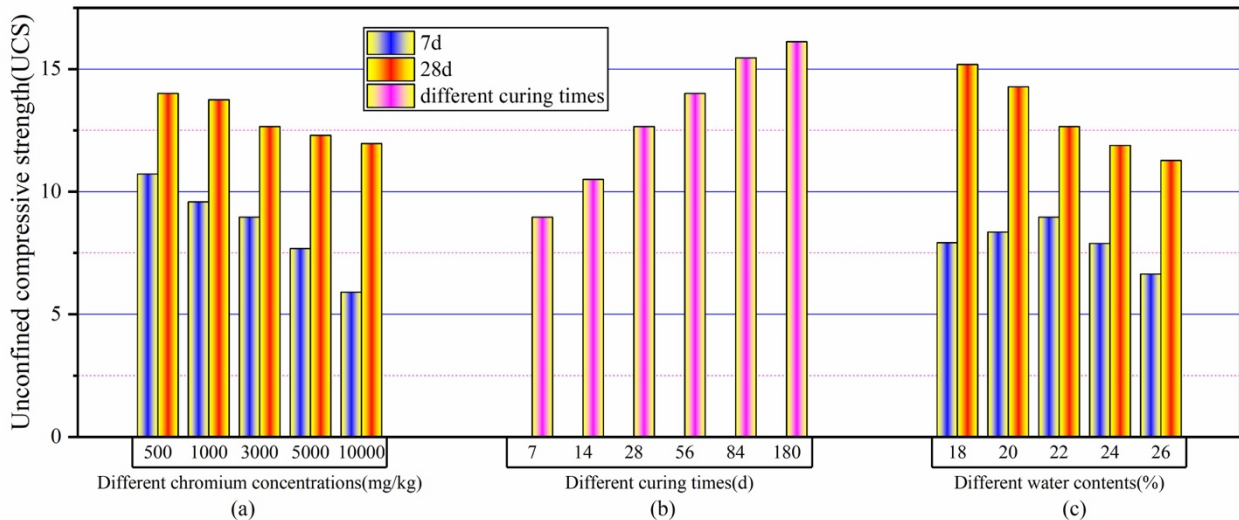


Fig. 1. The influence of different factors on UCS. (a) Different chromium concentrations. (b) Different curing ages. (c) Different water contents

4.2 Stress-strain relationship of chromium-contaminated soil after combined remediation

Uniaxial compressive strength is the most basic and important performance indicator of geotechnical materials. The stress-strain relationship under uniaxial compression of chromium-contaminated soil after combined remediation with composite preparation can fully reflect the deformation characteristics and destruction process at each stress stage. By averaging the three results for each group, the stress-strain relationship curves under different water contents, pollutant concentrations, and curing ages are obtained (Fig. 2).

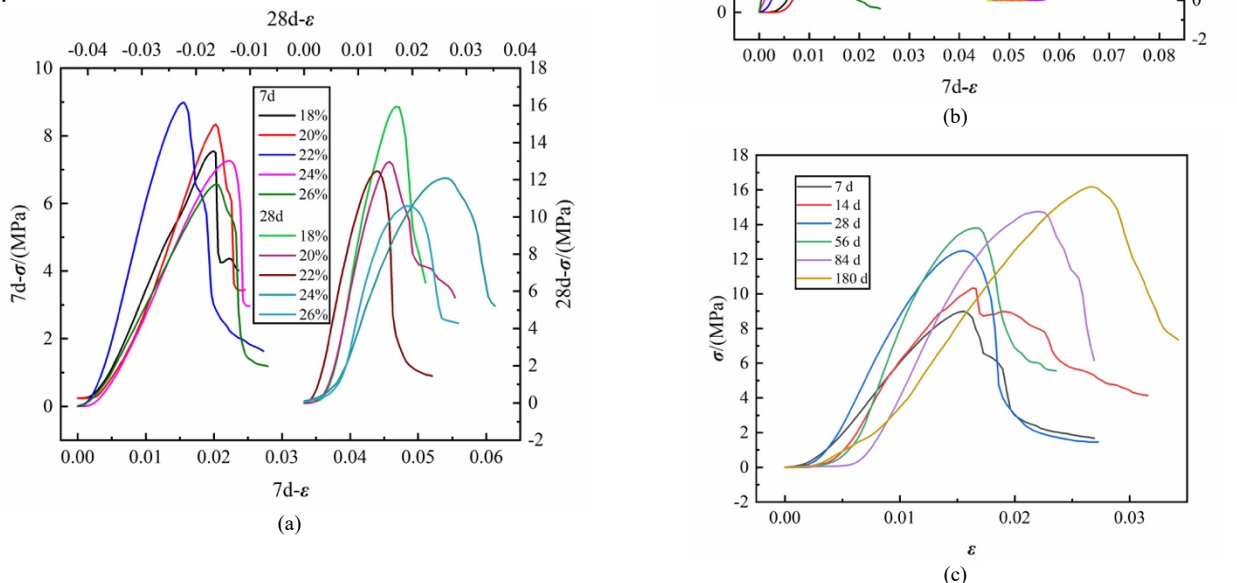


Fig. 2. Measured stress-strain relationship curve. (a) Different water contents. (b) Different chromium concentrations. (c) Different curing ages

According to Fig. 2, under the influence of different water contents, curing ages, and chromium concentrations, the stress-strain curves of chromium-contaminated soil after combined solidification-reduction-adsorption remediation have similar characteristics. A typical and complete simplified diagram of stress-strain curve, which can reflect the chromium-contaminated soil after combined remediation by the composite preparation, can be expressed as Fig. 3. The stress-strain curve can be divided into three stages (OA, AB, BC) and three regions (I, II, and III). The meanings of all variables in the Fig. 3 are explained where they are used.

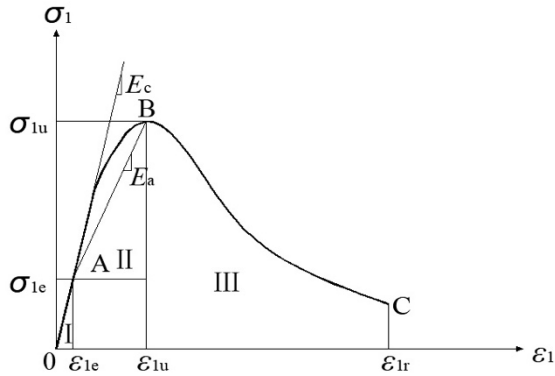


Fig. 3. Stress-strain curves of solidified soil specimens

Fig. 3 shows the stress-strain relationship curve of chromium-contaminated soil after combined remediation. The curve can be divided into three stages.

The first stage is the OA section, which is the initial straight-line section of the stress-strain curve of chromium-contaminated soil after remediation by the composite preparation. At this stage, a linear relationship exists between stress and strain. The specimens become loaded, the stress is small ($\sigma < \sigma_{1e}$), the strain increases approximately in proportion, the particles in the specimens are compressed, the voids are reduced, the particles are not damaged, and the particle deformation is within the range of linear elastic deformation. The specimen of chromium-contaminated soil after remediation shows linear elasticity. Hardening occurs in the chromium-contaminated soil after combined solidification-reduction-adsorption remediation.

The second stage is the AB section, where the stress-strain curve of chromium-contaminated soil repaired by the composite preparation shows a nonlinear ascending state. This stage starts from point A. As the stress gradually increases and when the stress exceeds the elastic limit (σ_{1e}) of the chromium-contaminated soil after remediation, the slope of the stress-strain relationship curve gradually decreases. At this time, the internal particles of the specimens are damaged, and the gaps between the particles are continuously compacted. This compaction effect has a sufficient advantage in the increase of strength compared to the reduction in strength caused by structural damage. At this stage, the specimen begins to suffer irreversible damage, and microcracks are generated inside the specimen. As the pressure increases, the particles of the specimen continue to undergo plastic destruction, and the stress reaches the peak at point B. The whole specimen is completely damaged. Macroscopically, the stress-strain curve shows a nonlinear rise, the internal cracks of the specimen expand outward, and obvious microcracks appear on the surface of the specimen.

The third stage is the BC section, where the stress-strain curve of the chromium-contaminated soil after remediation

decreases nonlinearly. At this stage, the specimen begins to be softened, that is, the stress decays rapidly when the strain increase is not great. After that, the stress-strain curve gradually changes from steep to slow, gradually reaching point C of the residual strength value. When the stress reaches the peak value, the cracks of the specimen continue to expand, extend, and connect, forming macroscopic oblique cracks along the weakest surface. As the strain increases, the crack gradually penetrates the full section, forming a damaged zone. While cracks in other parts of the specimen no longer propagate. The specimen has an external load that resists the frictional resistance of the inclined surface and the residual adhesive force, causing a slow decrease in the residual bearing capacity. After that, the specimen gradually transitions to a residual stage with a certain strength. When the strain reaches ϵ_{1r} , the residual strength is about $(0.2-0.4)\sigma_{1u}$. Under greater strain, the strength of the specimen is still not completely lost.

4.3 Constitutive equation of chromium-contaminated soil after combined remediation

Based on the stress-strain curve of the chromium-contaminated soil after combined solidification-reduction-adsorption remediation, the constitutive equation of chromium-contaminated soil is established as follows.

(1) Stress-strain constitutive equation of elastic straight line segment

As shown in Fig. 3, the corresponding stress and strain of point A on the OA segment are σ_{1e} and ϵ_{1e} respectively, where σ_{1e} is the elastic limit stress and ϵ_{1e} is the elastic limit strain. Equation (1) is as follows.

$$\epsilon_{1e} = \frac{\sigma_{1e}}{E_c} \quad (1)$$

In the equation, E_c is the elastic modulus of the chromium-contaminated soil after combined remediation by composite preparation. σ_{1e} is approximately $(0.3-0.4)\sigma_{1u}$, and σ_{1u} is the peak stress of the chromium-contaminated soil after remediation by composite preparation. The constitutive equation of the elastic straight section OA is shown in equation (2).

$$\sigma_1 = E_c \epsilon_1 (0 < \epsilon_1 < \epsilon_{1e}) \quad (2)$$

(2) Constitutive equation of the stress-strain relationship curve in the non-linear ascending stage

In order to better reflect the stress-strain relationship of the chromium-contaminated soil after combined solidification-reduction-adsorption remediation, and to make the constitutive equation more reasonable, the Popovics model [26] is introduced, as shown in equation (3).

$$\sigma_1 = \sigma_{1u} \frac{\epsilon_1}{\epsilon_{1u}} \frac{n}{n-1 + \left(\frac{\epsilon_1}{\epsilon_{1u}}\right)^n} \quad (3)$$

In the equation, ϵ_{1u} is the peak strain, σ_{1u} is the peak stress, and n is the model parameter. For the strain-softening stress-strain curve of the chromium-contaminated

soil after combined remediation, the curve can be divided into two parts, the ascending section and the descending section. In equation 3, the value of n is taken as n_a and n_b respectively. n is a parameter closely related to the stiffness of the material. The relationship between compressive strength and n can be established to express its physical meaning. The larger the value of n_a is, the steeper the ascending section of the curve in Fig. 3 is, indicating a larger initial modulus of the material. The larger the value of n_b is, the steeper the descending section of the curve in Fig. 3 is. Hence, the brittle failure of the material is more obvious.

Equation (3) can reflect the stress-strain relationship of the chromium-contaminated soil after combined remediation by composite preparation. However, when the parameter n is a fixed parameter, the fitting accuracy is low. As n is closely related to the stiffness of the material, the internal damage of the specimen gradually increases and small cracks appear in the specimen until it penetrates as the loading process of the specimen progresses. Therefore, the stiffness cannot be a constant but a constantly decreasing parameter. Using the damage mechanics method, the damage variable D is introduced. The damage variable is used to describe the damage change law. In this study, the trend that the elastic modulus decreases with increasing strain is fitted, and the equation (4) is obtained.

$$D = A \exp(\varepsilon_1) + B \tag{4}$$

$$\sigma_1 - \sigma_{1e} = (\sigma_{1u} - \sigma_{1e}) \frac{\varepsilon_1 - \varepsilon_{1e}}{\varepsilon_{1u} - \varepsilon_{1e}} \frac{n(1 - A \exp(\varepsilon) - B)}{n(1 - A \exp(\varepsilon) - B) - 1 + \left(\frac{\varepsilon_1 - \varepsilon_{1e}}{\varepsilon_{1u} - \varepsilon_{1e}}\right)^{n(1 - A \exp(\varepsilon) - B)}} \tag{10}$$

Namely,

$$\sigma_1 = (\sigma_{1u} - \sigma_{1e}) \frac{(\varepsilon_1 - \varepsilon_{1e})}{(\varepsilon_{1u} - \varepsilon_{1e})} \frac{n(1 - A \exp(\varepsilon) - B)}{n(1 - A \exp(\varepsilon) - B) - 1 + \left(\frac{\varepsilon_1 - \varepsilon_{1e}}{\varepsilon_{1u} - \varepsilon_{1e}}\right)^{n(1 - A \exp(\varepsilon) - B)}} + \sigma_{1e} \tag{11}$$

In the equation, if $m = \frac{\varepsilon_1 - \varepsilon_{1e}}{\varepsilon_{1u} - \varepsilon_{1e}}$ is made and m is substituted into equation (11), then equation (11) can be simplified to equation (12).

$$\sigma_1 = (\sigma_{1u} - \sigma_{1e}) \frac{mn(1 - D)}{n(1 - D) - 1 + m^{n(1 - D)}} + \sigma_{1e} \tag{12}$$

Taking the derivation on both sides of equation (12), equation 13 can be got.

$$\frac{d\sigma_1}{d\varepsilon_1} = \frac{E_a n(1 - D)(n(1 - D) - 1)[1 - m^{n(1 - D)}]}{[n(1 - D) - 1 + m^{n(1 - D)}]^2} \tag{13}$$

In the equation (13), according to the continuity of the curve, the equation (11) should satisfy the following boundary conditions.

- 1) When $\varepsilon_1 = \varepsilon_{1e}$, $m = 0$ and $\sigma_1 = \sigma_{1e}$.
- 2) When $\varepsilon_1 = \varepsilon_{1u}$, $m = 1$ and $\sigma_1 = \sigma_{1u}$.

In the equation, D is the damage variable. A and B are the parameters, which are determined by the test results. Introducing the damage variable of equation (4) into equation (3), and then equation (5) can be obtained.

$$\sigma_1 = \sigma_{1u} \frac{\varepsilon_1}{\varepsilon_{1u}} \frac{n(1 - A \exp(\varepsilon_1) - B)}{n(1 - A \exp(\varepsilon_1) - B) - 1 + \left(\frac{\varepsilon_1}{\varepsilon_{1u}}\right)^{n(1 - A \exp(\varepsilon_1) - B)}} \tag{5}$$

Equation (5) is the improved Popovics damage model.

For the AB ascending section, combine with Fig. 3 and set the following equation.

$$\sigma_{1u} = \sigma_{1u} - \sigma_{1e} \tag{6}$$

$$\sigma_1 = \sigma_1 - \sigma_{1e} \tag{7}$$

$$\varepsilon_{1u} = \varepsilon_{1u} - \varepsilon_{1e} \tag{8}$$

$$\varepsilon_1 = \varepsilon_1 - \varepsilon_{1e} \tag{9}$$

Substituting equations (6)-(9) into equation (5), the stress-strain constitutive equation of the chromium-contaminated soil after remediation in the AB ascending section can be obtained, as shown in equation (10).

3) When $\varepsilon_1 = \varepsilon_{1e}$, $m = 0$ and $\frac{d\sigma_1}{d\varepsilon_1} = \frac{E_a n(1 - D)}{n(1 - D) - 1} = E_c$, that is $E_a = \frac{n(1 - D) - 1}{n(1 - D)} E_c$.

4) When $\varepsilon_1 = \varepsilon_{1u}$, $m = 1$ and $\frac{d\sigma_1}{d\varepsilon_1} = 0$.

From this, the constitutive equation of the ascending section of the chromium-contaminated soil after combined remediation can be obtained, as shown in equation (14).

$$\sigma_1 = (\varepsilon_1 - \varepsilon_{1e}) E_a \frac{n(1 - D)}{n(1 - D) - 1 + \left(\frac{\varepsilon_1 - \varepsilon_{1e}}{\varepsilon_{1u} - \varepsilon_{1e}}\right)^{n(1 - D)}} + \varepsilon_{1e} E_c \tag{14}$$

(3) Constitutive equation of the stress-strain curve in the nonlinear descent stage

For the descending section BC, the damage evolution equation is fitted, as shown in equation (15).

$$D = A' + B' \varepsilon_1^{1.5} \tag{15}$$

In the equation, A' and B' are parameters, which are determined by the test results.

Introducing the damage variable, equation (16) is got.

$$\sigma_1 = \sigma_{1u} \frac{\varepsilon_1}{\varepsilon_{1u}} \frac{n(1-A'-B'\varepsilon_1^{1.5})}{n(1-A'-B'\varepsilon_1^{1.5})-1+\left(\frac{\varepsilon_1}{\varepsilon_{1u}}\right)^{n(1-D)}} \quad (16)$$

Let $m_b = \frac{\varepsilon_1}{\varepsilon_{1u}}$, $E_u = \frac{\sigma_{1u}}{\varepsilon_{1u}}$. Taking the derivation on both sides of equation (16), equation (17) is got.

$$\frac{d\sigma_1}{d\varepsilon_1} = \frac{1-m^{n(1-D)}}{\left[n(1-D)-1+m^{n(1-D)}\right]^2} E_u n(1-D)[n(1-D)-1] \quad (17)$$

From the continuity and boundary conditions, the following 4 points can be obtained.

- 1) When $\varepsilon_1 = \varepsilon_{1u}$, $m = 1$ and $\sigma_1 = \sigma_{1u}$.
- 2) When $\varepsilon_1 = \varepsilon_{1u}$, $m = 1$ and $\frac{d\sigma_1}{d\varepsilon_1} = 0$.
- 3) When $\varepsilon_1 \rightarrow \infty$, $m \rightarrow \infty$ and $\sigma_1 \rightarrow 0$.
- 4) When $\varepsilon_1 \rightarrow \infty$, $m \rightarrow \infty$ and $\frac{d\sigma_1}{d\varepsilon_1} \rightarrow 0$.

The constitutive equation of the descending section (BC) of the chromium-contaminated soil after combined remediation can be obtained, as shown in equation (18).

$$\sigma_1 = \varepsilon_1 E_u \frac{n(1-D)}{n(1-D)-1+\left(\frac{\varepsilon_1}{\varepsilon_{1u}}\right)^{n(1-D)}} \quad (18)$$

(4) Full stress-strain constitutive equation of chromium-contaminated soil after combined remediation by composite preparation

To obtain uniform formula, E_a in equation (14) is replaced with E_c , and E_u in equation (18) is replaced with E_c . Let $E_u = tE_c$, where t is a dimensionless constant.

A complete constitutive equation of the stress-strain curve for the chromium-contaminated soil after combined solidification-reduction-adsorption remediation can be obtained, as shown in equations (19a)-(19c).

$$\sigma_1 = E_c \varepsilon_1 (0 < \varepsilon_1 < \varepsilon_{1e}) \quad (19a)$$

$$\sigma_1 = E_c \left[\frac{(n(1-D)-1)\left(1-\frac{\varepsilon_{1e}}{\varepsilon_1}\right)}{(n(1-D)-1)+\left(\frac{\varepsilon_1-\varepsilon_{1e}}{\varepsilon_{1u}-\varepsilon_{1e}}\right)^{n(1-D)}} + \frac{\varepsilon_{1e}}{\varepsilon_1} \right] \varepsilon_1 \quad (19b)$$

$(\varepsilon_{1e} < \varepsilon_1 < \varepsilon_{1u})$

$$\sigma_1 = E_c \left[\frac{tn(1-D)}{(n(1-D)-1)+\left(\frac{\varepsilon_1}{\varepsilon_{1u}}\right)^{n(1-D)}} \right] \varepsilon_1 \quad (\varepsilon_{1u} < \varepsilon_1 < \infty) \quad (19c)$$

In the equation (19), E_c is the elastic modulus of the chromium-contaminated soil after remediation by composite preparation, $E_c = \frac{\sigma_{1e}}{\varepsilon_{1e}}$. E_u is the elastic modulus at the peak point of chromium-contaminated soil after remediation by composite preparation, $E_u = \frac{\sigma_{1u}}{\varepsilon_{1u}}$. σ_{1e} is the stress at the boundary point between the linear stage and the nonlinear stage in the stress-strain curve of chromium-contaminated soil after remediation by composite preparation, MPa. σ_{1u} is the stress corresponding to the peak point in the stress-strain curve of chromium-contaminated soil after remediation by composite preparation, MPa. ε_{1e} is the strain at the boundary point between the linear phase and the nonlinear phase in the stress-strain curve of chromium-contaminated soil after remediation by composite preparation. ε_{1u} is the strain corresponding to the peak point in the stress-strain curve of chromium-contaminated soil after remediation by composite preparation. n is the parameter. D is the damage variable. All parameters in the model can be obtained directly or indirectly through compressive strength tests.

4.4 Verification of constitutive equation

Measurement data was used to verify the theoretical value of the uniaxial compression stress-strain constitutive equation (Figs. 4, 5, and 6).

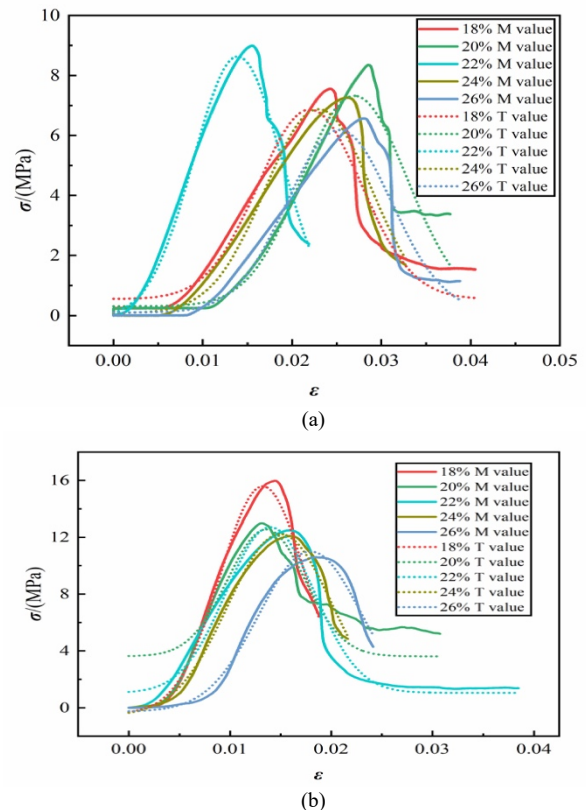
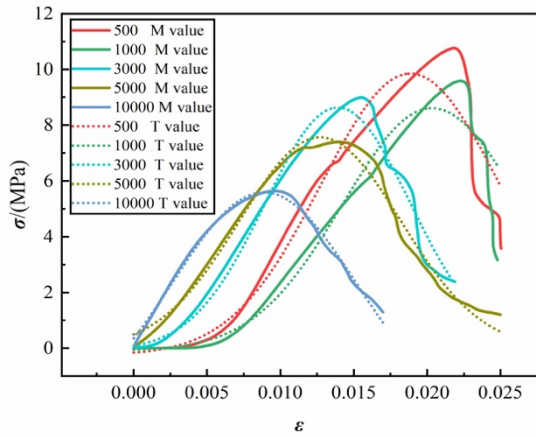
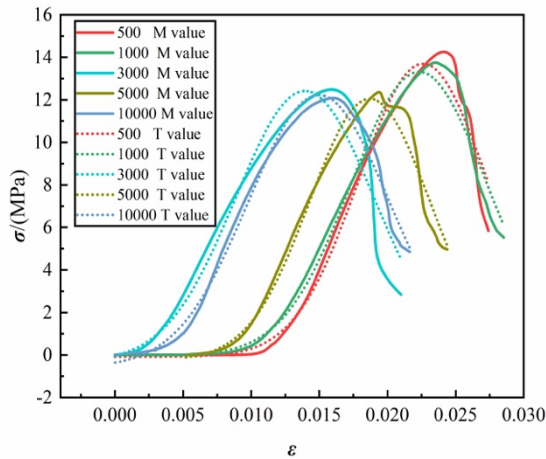


Fig. 4. Validation results of the stress-strain constitutive model under different water contents. (a)7d. (b)28d



(a)



(b)

Fig. 5. Validation results of the stress-strain constitutive model under different chromium concentrations. (a)7d. (b)28d

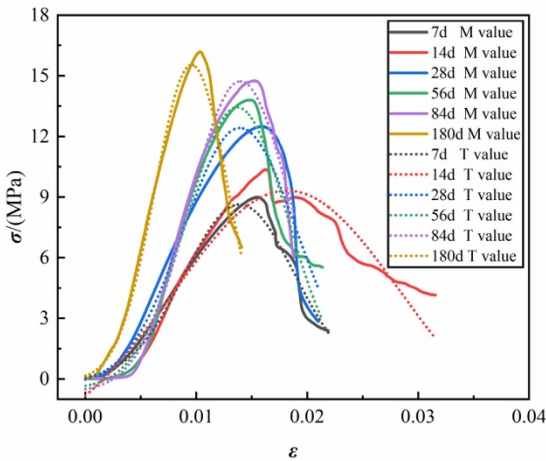


Fig. 6. Validation results of the stress-strain constitutive model under different curing ages

From the above comparison results, the theoretical calculation results of chromium-contaminated soil after combined solidification-reduction-adsorption remediation fit well with the ascending and descending sections of the measured stress-strain relationship curve under different water contents, curing ages and chromium concentrations, without significant errors. The verification results show that the stress-strain constitutive model derived in this study can better reflect the stress-strain relationship of the chromium-contaminated soil after combined solidification-reduction-adsorption remediation.

5. Conclusions

In this study, solidified specimens were prepared using the chromium-contaminated soil after remediation of calcium polysulfide, synthetic zeolite from fly ash, and cement. The strength characteristics under different water contents, chromium concentrations, and curing ages were studied, and the stress-strain curves under different conditions were obtained. Based on the damage mechanics, the damage variables were introduced. The constitutive model of the chromium-contaminated soil after combined remediation was established, and the theoretical values were verified by the experimental data. The obtained conclusions are as follows.

(1) The UCS of the solidified body after 7 d of curing age increases first and then decrease, while the UCS of the solidified body after 28 d of curing age continues to decrease. UCS shows a continuous growth trend with increasing curing ages due to the delayed effect of hydration and pozzolanic reaction. Chromium with high concentrations has a significant weakening effect on the strength of solidified soil, resulting in a decrease in UCS.

(2) Based on the analysis of stress-strain curves under different conditions, in the initial stage, the solidified body undergoes linear elastic deformation and hardening. The stress-strain curve shows a non-linear ascending state. The irreversible damage gradually appears at the specimen, and the specimen suffers plastic failure. After reaching the peak stress, the strain softening phenomenon gradually decreases. The solidified body has an obvious elastic stage under loading, and the plastic deformation is also relatively large.

(3) The damage variable was introduced, the *Popovics* model was improved, and the elastoplastic nonlinear constitutive model of chromium-contaminated soil after combined remediation was established. This model can accurately describe the stress-strain relationship of solidified bodies with different water contents, curing ages and chromium concentrations under uniaxial compression.

(4) The constitutive model was verified. The calculated values of the model fits well with the test values, indicating that the established constitutive model was reasonable.

The obtained conclusions can be extended to the constitutive model of solidified bodies of chromium-contaminated soil and provide a theoretical basis for the engineering application of heavy metal-solidified bodies. Although we introduced the damage variable to make the constitutive model of heavy metal-contaminated soil more accurate, it still lacks real practical application. In the future, we expect this model to be widely used in the theoretical study of chromium-contaminated solids, and even extended to other heavy metal-contaminated solids.

Acknowledgements

The authors are grateful for the support provided by the Scientific Research Project of Educational Department of Liaoning Province of China (No. LJKZ0344), the Liaoning Provincial Natural Science Foundation of China (No. 2019-ZD-0037), and the Liaoning BaiQianWan Talents Program (Grant No. 2018C01).

This is an Open Access article distributed under the terms of the Creative Commons Attribution License.



References

1. Khalid, S., Shahid, M., Niazi, N. K., Murtaza, B., Bibi, I., Dumat, C., "A comparison of technologies for remediation of heavy metal contaminated soils". *Journal of Geochemical Exploration*, 182(B), 2017, pp.247-268.
2. Li, X., Yu, X., Liu, L., Yang, J., "Cyclic drying and wetting tests on combined remediation of chromium-contaminated soil by calcium polysulfide, synthetic zeolite and cement". *Scientific Reports*, 11, 2021, pp.11643.
3. Wang, F., Zhang, Y., Shen, Z., Pan, H., Xu, J., Al-Tabbaa, A., "GMCs stabilized/solidified Pb/Zn contaminated soil under different curing temperature: leachability and durability". *Environmental Science and Pollution Research*, 26, 2019, pp.26963-26971.
4. Fitch, J. R., Cheeseman, C. R., "Characterisation of environmentally exposed cement-based stabilised/solidified industrial waste". *Journal of Hazardous Materials*, 101(3), 2003, pp.239-255.
5. Li, X., Tong, Z., Liu, L., Yu, X., Meng, D., "Influence of freeze-thaw cycles on the strength and leaching characteristics of chromium-contaminated soil repaired by reduction-solidification/stabilization". *Journal of Engineering Science and Technology Review*, 14(1), 2021, pp.61-70.
6. Vatsala, A., Nova, R., Srinivasa Murthy, B. R., "Elastoplastic model for cemented soils". *Journal of Geotechnical and Geoenvironmental Engineering*, 127(8), 2001, pp.679-687.
7. Li, H., Feng, S., Wei, L., Chen, Z., "Time effect of pile-soil interaction and its elastic-viscoplastic constitutive model". *Rudarsko-geološko-naftni zbornik*, 34(1), 2019, pp.1-11.
8. Zhou, S., Xia, C., Zhao, H., Mei, S., Zhou, Y., "Statistical damage constitutive model for rocks subjected to cyclic stress and cyclic temperature". *Acta Geophys*, 65, 2017, pp.893-906.
9. Chong, S., "Development of constitutive model for simulation of cemented soil". *Geotechnical and Geological Engineering*, 37, 2019, pp.4635-4641.
10. Zhi, B., Wang, P., Liu, E., Liu, W., "A constitutive model for structured loess under high stress conditions". *Iranian Journal of Science and Technology, Transactions of Civil Engineering*, 44(4), 2020, pp.461-470.
11. Tu, B., Liu, L., Cheng, K., Zhang, B., Zhao, Y., Yang, Q., Song, K., "A constitutive model for cemented tailings backfill under uniaxial compression". *Frontiers in Physics*, 8, 2020, pp. 173.
12. Yao, Y., Liu, L., Luo, T., "A constitutive model for granular soils". *Science China Technological Sciences*, 61(10), 2018, pp.1546-1555.
13. Bathayian, M. H., Maleki, M., "Adaptation of an existing constitutive model for describing mechanical behaviour of cemented granular soils". *Geomechanics and Geoengineering*, 13(3), 2018, pp.184-197.
14. Wang, P., Liu, E., Zhi, B., Song, B., "A macro-micro viscoelastic-plastic constitutive model for saturated frozen soil". *Mechanics of Materials*, 147, 2020, pp.103411.
15. Pan, Y., Zhao, Z., He, L., Wu, G., "A nonlinear statistical damage constitutive model for porous rocks". *Advances in Civil Engineering*, 2020.
16. Cao, C., Zhu, Z., Fu, T., Liu, Z., "A constitutive model for frozen soil based on rate-dependent damage evolution". *International Journal of Damage Mechanics*, 27(10), 2018, pp.1589-1600.
17. Xie, Q., Su, L., Zhu, Z., "Dynamic constitutive model of frozen soil that considers the evolution of volume fraction of ice". *Scientific Reports*, 10, 2020, pp.20941.
18. Abioghli, H., Hamidi, A., "A constitutive model for evaluation of mechanical behavior of fiber-reinforced cemented sand". *Journal of Rock Mechanics and Geotechnical Engineering*, 11(02), 2019, pp.349-360.
19. Doherty, J. P., Wood, D. M., "A bonding and damage constitutive model for lightly cemented granular material". *Computers and Geotechnics*, 127, 2020, pp.103732.
20. Liu, H., Li, L., Zhao, S., Hu, S., "Complete stress-strain constitutive model considering crack model of brittle rock". *Environmental Earth Sciences*, 78, 2019, pp.629.
21. Ke, H., Chen, Y., Dong, D., Guo, C., Feng, S., "Non-linear elastic model for MSW considering dilatancy effect". *Environmental Geotechnics*, 6(3), 2019, pp.125-136.
22. Tachibana, S., Ito, S., Iizuka, A., "Constitutive model with a concept of plastic rebound for expansive soils". *Soils and Foundations*, 60(1), 2020, pp.179-197.
23. Luo, J., Zhang, H., Yang, J., "Hydrothermal synthesis of sodalite on alkali-activated coal fly ash for removal of lead ions". *Procedia Environmental Sciences*, 31, 2016, pp.605-614.
24. Zha, F., Zhu, F., Kang, B., Xu, L., Deng, Y., Yang, C., Chu, C., "Experimental investigation of cement/soda residue for solidification/stabilization of Cr-contaminated soils". *Advances in Civil Engineering*, 2020.
25. Mukiza, E., Zhang, L., Liu, X., "Durability and microstructure analysis of the road base material prepared from red mud and flue gas desulfurization fly ash". *International Journal of Minerals, Metallurgy and Materials*, 27, 2020, pp.555-568.
26. Mander, J. B., Priestley, M. J. N., Park, R., "Theoretical stress-strain model for confined concrete". *Journal of Structural Engineering*, 144(8), 1988, pp.1804-1826.